Biochemistry and Biophysics Reports 34 (2023) 101440

Contents lists available at ScienceDirect

Biochemistry and Biophysics Reports

journal homepage: www.elsevier.com/locate/bbrep

A prediction model for prognosis of gastric adenocarcinoma based on six metabolism-related genes

Jingyu Zhao [a,b,c], Yu Liu [b,c,d], Qianwen Cui [b,c,d], Rongli He [e], Jia-Rong Zhao [c], Li Lu [e], Hong-Qiang Wang [d,f], Haiming Dai [b,c,d], Hongzhi Wang [b,c,d], Wulin Yang [b,c,d,*]

[a] Institutes of Physical Science and Information Technology, Anhui University, Hefei, 230601, China
[b] Anhui Province Key Laboratory of Physics and Technology, Institute of Health & Medical Technology, Hefei Institutes of Physical Science, Chinese Academy of Sciences, Hefei, 230031, China
[c] Hefei Cancer Hospital, Chinese Academy of Sciences, Hefei, 230031, China
[d] Science Island Branch, Graduate School of USTC, Hefei, 230026, China
[e] Department of Anatomy, Shanxi Medical University, Taiyuan, 030024, China
[f] Biological Molecular Information System Laboratory, Institute of Intelligent Machines, Hefei Institutes of Physical Science, Chinese Academy of Sciences, Hefei, 230031, China

ARTICLE INFO

Keywords:
Gastric adenocarcinoma
Metabolism-related genes
Prognostic model
Immunohistochemistry
Survival analysis

ABSTRACT

Background: The study of tumor metabolism is of great value to elucidate the mechanism of tumorigenesis and predict the prognosis of patients. However, the prognostic role of metabolism-related genes (MRGs) in gastric adenocarcinoma (GAD) remains poorly understood.

Methods: We downloaded the gene chip dataset GSE79973 (n = 20) of GAD from the Gene Expression Omnibus (GEO) database to compare differentially expressed genes (DEGs) between normal and tumor tissues. We then extracted MRGs from these DEGs and systematically investigated the prognostic value of these differential MRGs for predicting patients' overall survival by univariable and multivariable Cox regression analysis. Six metabolic genes (ACOX3, APOE, DIO2, HSD17B4, NUAK1, and WHSC1L1) were identified as prognosis-associated hub genes, which were used to build a prognostic model in the training dataset GSE15459 (n = 200), and then validated in the dataset GSE62254 (n = 300).

Results: Patients were divided into high-risk and low-risk subgroups based on the model's risk score, and it was found that patients in the high-risk subgroup had shorter overall survival than those in the low-risk subgroup, both in the training and testing datasets. In addition, for the training and testing cohorts, the area under the ROC curve of the prognostic model for one-year survival prediction was 0.723 and 0.667, respectively, indicating that the model has good predictive performance. Furthermore, we established a nomogram based on tumor stage and risk score to effectively predict the overall survival (OS) of GAD patients. The expression of 6 MRGs at the protein level was confirmed by immunohistochemistry (IHC). Kaplan-Meier survival analysis further confirmed that their expression influenced OS in GAD patients.

Conclusion: Collectively, the 6 MRGs signature might be a reliable tool for assessing OS in GAD patients, with potential application value in clinical decision-making and individualized therapy.

1. Introduction

According to the latest survey in 2020, gastric cancer is the fifth most common cancer with 5.6% of new cases worldwide and the fourth most common death-causing cancer with a mortality rate of 7.7% [1]. Gastric cancer is one of the leading causes of cancer-related death in Asian countries and the second most common cancer in China, with approximately 403,000 new cases (281,000 in men and 122,000 in women) in 2015 [2]. Of all malignant tumors originating in the stomach, gastric adenocarcinoma (GAD) is the most common histological type (~95%) [3]. Currently, the diagnosis of GAD mainly depends on histopathological examination, serum biomarkers and imaging evaluation. Because

* Corresponding author. Institute of Health and Medical Technology, Hefei Institutes of Physical Science, CAS, No. 350, Shushanhu Road, Hefei, 230031, Anhui, China.
E-mail address: yangw@cmpt.ac.cn (W. Yang).

https://doi.org/10.1016/j.bbrep.2023.101440
Received 23 December 2022; Received in revised form 10 February 2023; Accepted 13 February 2023
2405-5808/© 2023 The Authors. Published by Elsevier B.V. This is an open access article under the CC BY-NC-ND license (http://creativecommons.org/licenses/by-nc-nd/4.0/).

the early symptoms are not obvious, most patients with GAD are already in the advanced stage when diagnosed. Early detection of GAD is still a clinical challenge, which may also be a reason for the high mortality rate of GAD patients.

The TNM staging system commonly used in clinical practice can predict the prognosis of GAD patients according to different stages [4]. However, patients at the same stage can have different outcomes [5]. Moreover, there are contradictions between different histopathological classifications [6]. Therefore, there is a need to develop a more effective method to predict the prognosis of GAD and to provide a reference for subsequent individualized treatment. Molecular predictive models are one of the solutions and much research has been done in gastric cancer. For example, a molecular prediction system was applied to the prediction of peritoneal recurrence after radical gastrectomy [7]; An immune score-based model predicts postoperative survival and adjuvant chemotherapy choice in patients with gastric cancer [8]. However, most of these studies lack sufficient testing cohorts or are not consistent enough and have not been applied in clinical practice [9,10].

Metabolic reprogramming is one of the important features of cancer. The relationship between metabolism and tumorigenesis involves complex biological processes and molecular regulation [11]. Gastric cancer also follows the Warburg effect, which enables cancer cells to maintain growth under hypoxia, provides raw materials for cell biosynthesis and division, and maintains intracellular redox homeostasis [12]. These functions are also related to the occurrence, proliferation, invasion, and metastasis of gastric cancer cells. In addition to the Warburg effect, abnormal glucose metabolism is often accompanied by changes in lipid and amino acid metabolism, presenting as a general increase in lipid and triglyceride levels [13], or fluctuations in the concentrations of different amino acids, such as significantly decreased leucine level and significantly increased glycine, phenylalanine, and arginine levels in gastric cancer [14].

In view of the importance of metabolism in tumor development, attempts have been made to construct prognostic model of GAD using metabolic genes [15]. However, in Luo et al.'s study, the area under ROC curve (AUC) of both the training queue and the internal testing queue was lower than 0.7, indicating that the predictive performance of the model was poor and there were still some deficiencies to be improved. In this study, we first extracted more comprehensive metabolic genes from the VHM (The Virtual Metabolic Human) database and then analyzed their differential expression in tumor and normal tissues to obtain characteristic metabolic genes as parameters in an attempt to establish a better prognostic model.

2. Materials and methods

2.1. Sample collection

Tissue wax block samples of GAD were collected in the Department of Pathology, Hefei Cancer Hospital, Chinese Academy of Sciences. This contained 8 patients, including 2 gastritis patients and 6 GAD patients, totally 8 pairs of samples for immunohistochemistry. All of these patients were diagnosed by pathological diagnosis between January 2020 and December 2020. This study was approved by the institutional ethics review committee of Hefei Institutes of Physical Science, Chinese Academy of Sciences (Approval number: Y-2020-11).

2.2. Data processing

From a GEO database (https://www.ncbi.nlm.nih.gov/geo/) to download three independent data sets, including GSE79973 (n = 20), GSE15459 (n = 200), GSE62254 (n = 300), a total of 520 patients with GAD were included. All three datasets were processed using the same on-chip platform GPL570 (Affymetrix Human Genome U133 Plus 2.0 Array, Santa Clara, CA, USA). GSE79973 contained ten pairs of tumor and normal tissues for differential gene expression analysis. GSE15459 was used as the training cohort for modeling, while GSE62254 was used as the testing cohort.

2.3. Identification of differentially expressed MRGs in GAD

Previous studies suggested that biomarkers based on differentially expressed DEGs between tumors and adjacent normal tissues can better predict the prognosis of cancer. To screen potential biomarkers, the 'limma' package in R was used in this study to analyze DEGs by comparing paired tumor and normal tissues in GSE79973. These DEGs were intersected with MRGs derived from the VMH database (VMH, www.vmh.life), and then the differentially expressed MRGs obtained were further analyzed.

2.4. Prognostic model construction

Univariable Cox regression analysis was performed on the training cohort GSE15459 with 200 samples. According to a P-value less than 0.001, 16 metabolic genes associated with survival were identified (APOE, ATP5F1, CBX1, CYP4F12, DIO2, GAK, HSD17B4, LOX, MAP4K4, NUAK1, PDE3A, SCP2, SLC25A20, TGM2, WHSC1L1). Based on preliminarily selected prognostic genes, we established a multivariable Cox proportional risk regression model to predict the prognosis of patients with GAD and calculate the risk score. In this model, the risk score of each sample is calculated as follows:

$$Risk\ score = \sum_{i=1}^{n} Exp_i \alpha_i,$$

where α is the regression coefficient and Exp is the gene expression value.

2.5. Evaluating the prognostic performance of the model

To evaluate the performance of the prognostic model, we divided GAD patients in the training cohort GSE15459 into low- and high-risk subgroups according to the median risk score and drew the Kaplan-Meier survival curve, and then compared the difference in overall survival (OS) between the two subgroups by log-rank test. In addition, we used the 'SurvivalRoc' package to construct the ROC curve and draw the nomogram graph to predict overall survival. Furthermore, to confirm the predictive value of the model, we also drew the Kaplan-Meier survival curves, ROC curves for the testing cohort.

2.6. Immunohistochemistry

Formalin-fixed paraffin-embedded tissue was cut into 3 μm thick sections and collected with adhesive slides. The paraffin-embedded GAD tissues and surrounding tissues were dewaxed by xylene and ethanol, and then the antigens were recovered by a high-pressure repair method. The slides were sealed with serum at 37 °C for 30 min, incubated overnight with primary anti-DIO2 antibody (1:2000, from Wuhan Sanying Biotechnology Co., Ltd., item No. Cat No. 66813-1-Ig) at 4 °C, and subsequently incubated with secondary antibody at room temperature for 30 min. The slides were counterstained for 30 s with hematoxylin and finally sealed. Immunohistochemical results were independently evaluated by two experienced pathologists. Some immunohistochemical results of other genes in the model will be obtained from the HPA database [16] (https://www.proteinatlas.org/).

2.7. Statistical analysis

All statistical analyses in this study were based on version R4.1.0 (https://www.r-project.org/). The log-rank test was used to test the difference in survival rate, and the Kaplan-Meier survival curve was drawn. $P < 0.05$ was considered statistically significant.

3. Results

3.1. Screening of differentially expressed MRGs in GAD

The workflow of this study is shown in Fig. 1A. Gene expression on-chip data and corresponding clinical information of patients with GAD were downloaded from the GEO database. The 'limma' package was used to analyze the DEGs in the GSE79973 dataset which contains 10 pairs of tumor and adjacent normal tissues ($P < 0.05$, $|\log2FC| \geq 1.0$). After intersecting the DEGs with 3695 MRGs extracted from the VMH database (https://www.vmh.life), 310 differentially expressed MRGs were obtained.

3.2. Selection of prognostic related MRGs

Univariable Cox regression analysis was performed on the training cohort GSE15459 (n = 200), and a total of 16 prognosis-related hub MRGs significantly associated with survival were selected ($P < 0.001$) (Fig. 1B), including ACOX3, APOE, ATP5F1, CBX1, CYP4F12, DIO2, GAK, HSD17B4, LOX, MAP4K4, NUAK1, PDE3A, SCP2, SLC25A20, TGM2, and WHSC1L1. Next, multivariable Cox regression analyses were performed on the 16 genes to investigate their effects on patient survival and clinical outcomes. 6 hub MRGs, including ACOX3, APOE, DIO2, HSD17B4, NUAK1, and WHSC1L1 (Fig. 1C), were identified as independent predictors in GAD patients. APOE, DIO2, and NUAK1 were upregulated genes, while ACOX3, HSD17B4, and WHSC1L1 were downregulated genes. Among all 6 independent prognostic genes, the P-value of DIO2 was the smallest ($P = 0.005$), suggesting its important role in the prognosis of GAD.

3.3. Construction and analysis of prognostic model

6 hub MRGs identified by multivariable stepwise Cox regression were used to construct the prognostic model. The risk score for each patient was calculated by the following formula:

Risk score =(-0.7124*ACOX3) + (0.2715*APOE) + (0.3697*DIO2)+ (−0.8258*HSD17B4) + (0.4775*NUAK1) + (−1.0427*WHSC1L1)

The predictive ability of the model was then evaluated by survival analysis, and 300 GAD patients in the training cohort were divided into low- and high-risk groups according to the median risk score. The results showed that the survival time of patients in the high-risk group was significantly shorter than that in the low-risk group (Fig. 2A). To further assess the prognostic ability of the model, a time-dependent ROC curve was generated. In the training cohort, the area under the ROC curve for overall survival was 0.723 at 1 year, 0.767 at 3 years, and 0.775 at 5 years (Fig. 2B), indicating a favorable diagnostic performance. Fig. 2C shows the expression heatmaps of the 6 MRGs, patient survival status, and risk scores of each case in the low- and high-risk groups. In addition, to assess whether the predictive model had a similar prognostic value in other cohorts of GAD patients, a testing cohort GSE62254 was applied for validation. In the testing cohort, patients with a high risk score also had worse overall survival than those with a low risk score (Figs. S1A and C). The area under the ROC curve for overall survival was 0.667 at 1 year, 0.640 at 3 years, and 0.623 at 5 years (Fig. S1B). The above results suggest that this prognostic model has a good predictive ability.

3.4. The risk score of the model is an independent prognostic factor

In addition, univariable and multivariable Cox regression analyses were used to evaluate the prognostic significance of different clinical features in GAD patients in the training cohort. Age, gender, lauren type, tumor stage, and risk score of the model were included in the prognostic analysis related to survival time. Univariable (Fig. 3A) and multivariable (Fig. 3B) Cox regression analyses revealed that tumor stage and risk score were consistently independent prognostic factors associated with overall survival in the training cohort ($P < 0.001$) (Table S1).

3.5. Construction of nomogram

To make the results of the predictive model more readable and

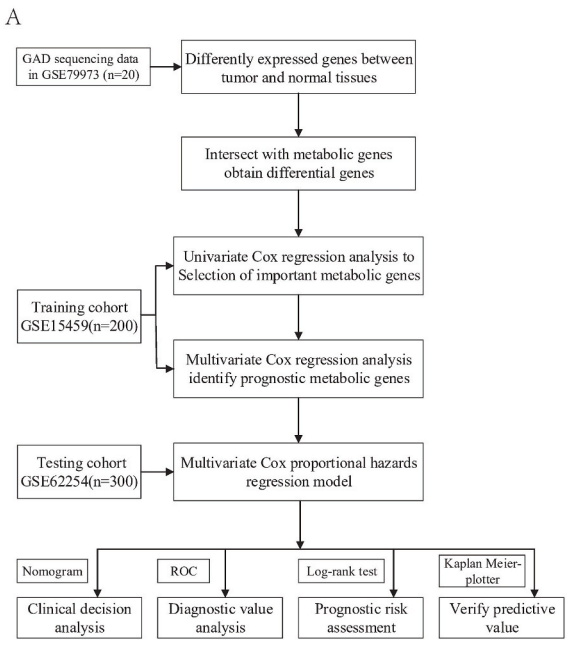

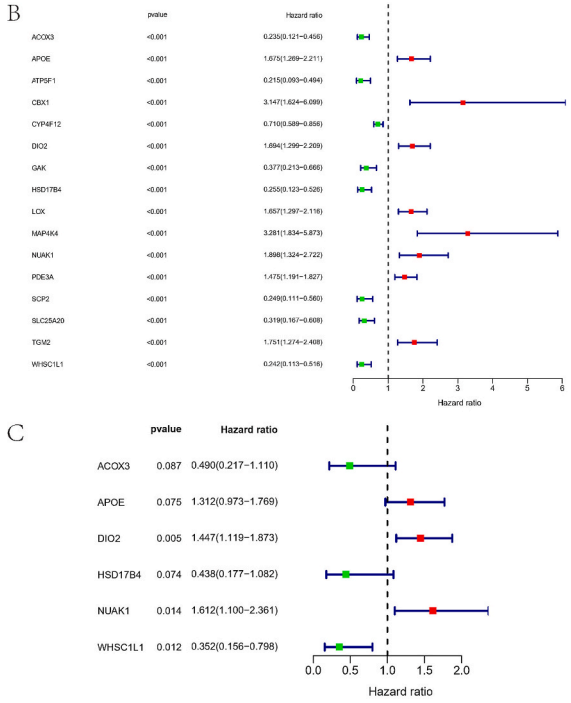

Fig. 1. A, Flow chart of the prognostic model's construction and its validation. B, 16 prognosis-related MRGs were identified by univariable Cox regression analysis. C, Multivariable Cox regression analysis identified 6 independent prognosis-related MRGs.

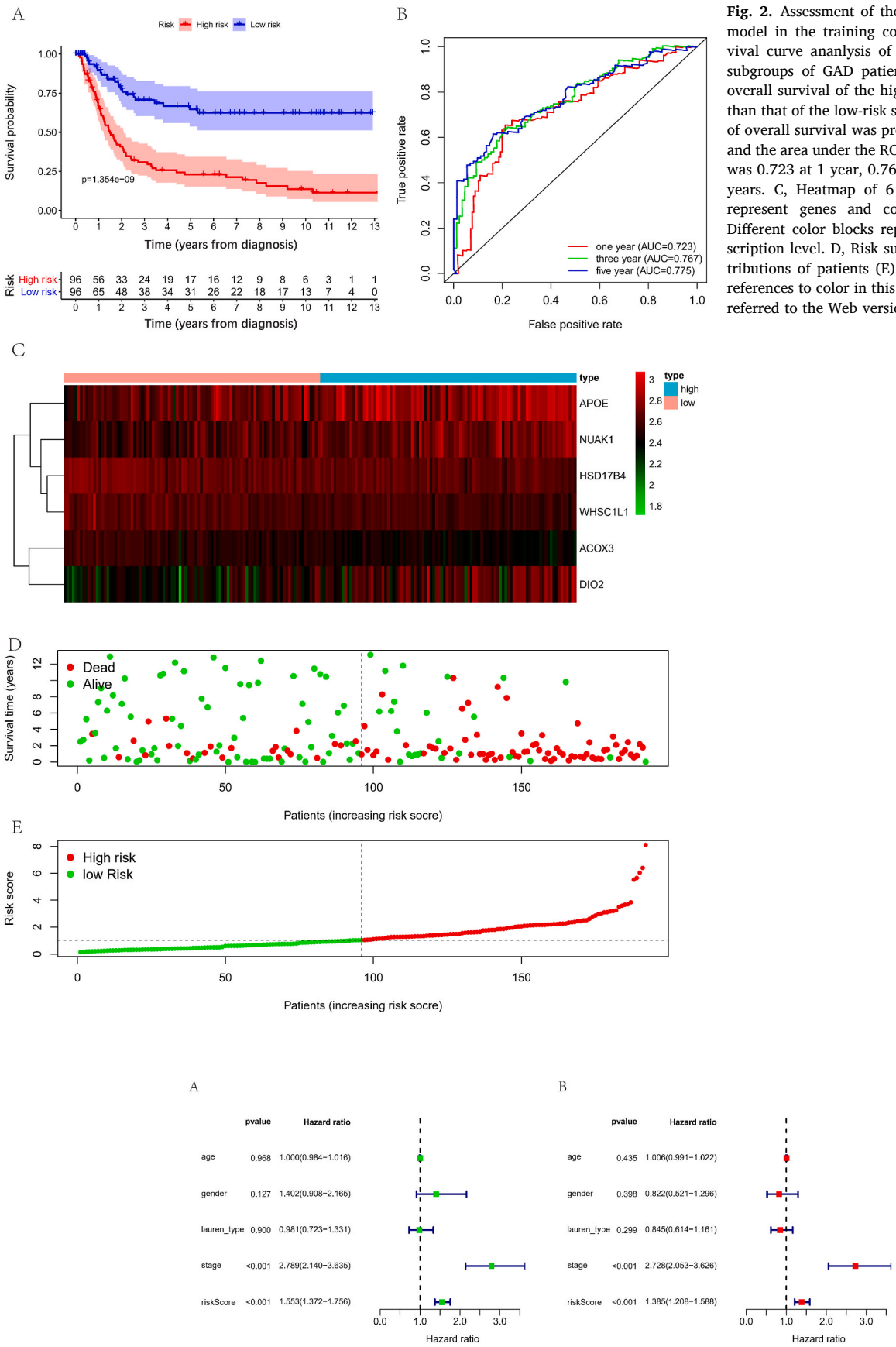

Fig. 2. Assessment of the 6 MRGs-based prognostic model in the training cohort. A, Kaplan-Meier survival curve ananlysis of the low-risk and high-risk subgroups of GAD patients in the training cohort, overall survival of the high-risk subgroup was lower than that of the low-risk subgroup. B, The ROC curve of overall survival was predicted based on risk score, and the area under the ROC curve for overall survival was 0.723 at 1 year, 0.767 at 3 years and 0.775 at 5 years. C, Heatmap of 6 MRGs' expressions. Rows represent genes and columns represent patients. Different color blocks represent differences in transcription level. D, Risk survival status and score distributions of patients (E). (For interpretation of the references to color in this figure legend, the reader is referred to the Web version of this article.)

Fig. 3. Assessment of independent prognostic factors. Univariable (A) and multivariable (B) analyses of the training cohort was based on risk scores and other clinical features (including age, sex, Lauren typing, and T stage).

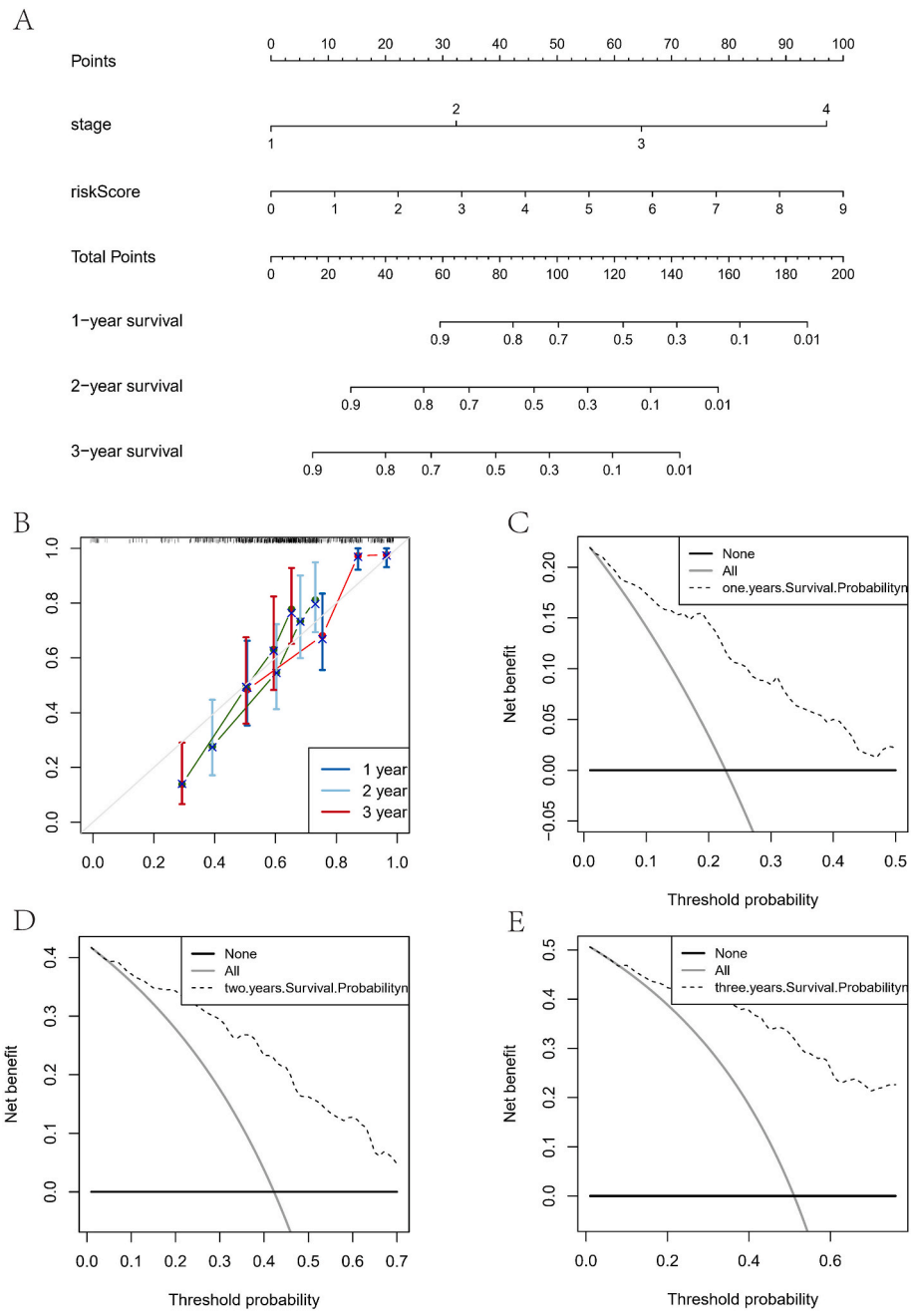

Fig. 4. Construction of the nomogram. The tumor stage and the risk score in the training cohort (A) was integrated to predict the survival probability of patients at 1, 2, and 3 years. The score was assigned by vertical line upward for the expression value of each gene, then the score was added together to get the total score. The survival probability of patients in 1, 2, and 3 years was predicted by vertical line downward from the total score. (B) The calibration curve of the model was established based on the consistency between the predicted results and the observed outcomes at 1, 2 and 3 years. Close-ended vertical lines represent the 95% confidence intervals. The x-axis indicates predicted survival probability, and the y-axis indicates the actual freedom from DFS for the patients. The relative 45-degree line indicates an ideal performance of a nomogram. (C–E) Decision curve analysis of the nomogram. The x-axis represents the percentage of threshold probability, and the y-axis represents the net benefit. The black lines represent the assumption that no patients relapsed at 1 (C), 2(D), or 3 years (E). The gray lines represent the assumption that all patients relapsed. The dotted lines represent the performance of nomogram.

facilitate the evaluation of patient prognoses, we integrated tumor stage and risk score to established a nomogram (Fig. 4A). We assigned points to each variable according to the coefficient of each variable on survival in the model. For each independent variable, a horizontal line was drawn to determine the point and add the points of all variables together to obtain the total score. The 1-, 2-, and 3-years survival rates of patients with GAD can be estimated, which will facilitate clinical decision-making and patient prognosis management. Calibration plots indicated that the nomogram performed well compared with an ideal model (Fig. 4B). The DCA curve indicated that most of GAD patients are suitable for survival prediction with this nomogram, showing its wide applicability (Fig. 4C, D, E).

3.6. *Verification of protein expression of 6 hub MRGs in tissues*

The immunohistochemical statuses of the hub MRGs were checked on the HPA website. Among them, ACOX3, APOE, HSD17B4 and WHSC1L1 had queryable immunohistochemical results, and the protein expression changes were consistent with the results of gene expression analysis. APOE was upregulated in tumor tissues (Fig. 5A), while ACOX3, HSD17B4, and WHSC1L1 were downregulated (Fig. 5B, C, D).

DIO2 had the smallest p-value in multivariable Cox analysis, suggesting that DIO2 may be the key factor related to the prognosis of GAD. Immunohistochemical staining was performed on DIO2 and the results showed that DIO2 protein was located mainly in the cytoplasm of GAD cells (Fig. 5E, F, G). Compared with the corresponding noncancerous adjacent tissues, the expression level of the DIO2 gene was higher in GAD tissues. Interestingly, the expression level of DIO2 protein was also significantly correlated with the proliferation of gastric gland cells, as it was correlated with KI67 staining and was strongly expressed in reactive hyperplasia glands (Fig. 5E, F, G). The above results indicated that the changes in the protein expression of 6 hub MRGs were consistent with

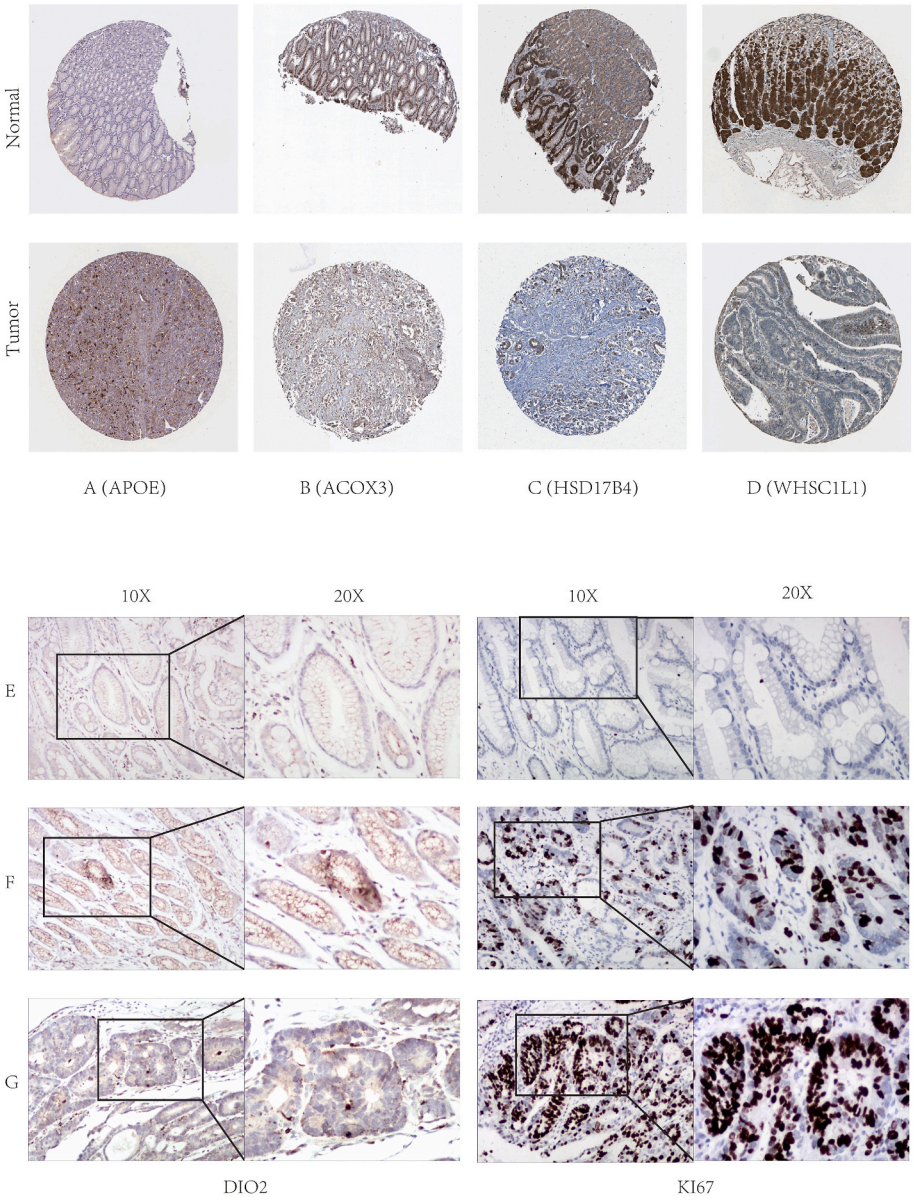

Fig. 5. The protein expressions of 6 MRGs. The changes of protein expressions of APOE (A), ACOX3 (B), HSD17B4 (C), and WHSC1L1 (D) were consistent with that of mRNA expressions. The expression of APOE was significantly increased in GAD, while ACOX, HSD17B4 and WHSC1L1 were relatively downregulated in cancer tissues. Protein expression of DIO2 and KI67 in different cell sources, including normal glands (E), reactive hyperplasia glands (F), and cancer cells. (G). Each photo was photographed with 10X and 20× magnification with light microscopy, respectively. DIO2 staining was upregulated in both the reactive hyperplasia glands and cancerous tissues compared with the normal tissues.

those of mRNA expression and the DIO2 may play an essential role in abnormal cell proliferation.

3.7. Validation of the prognostic value of hub MRGs

To further explore the prognostic value of the 6 MRGs in GAD, the tool of Kaplan-Meier Curves was used to determine the relationship between MRGs and overall survival (Fig. 6). Log-rank test results showed that these 6 MRGs were significantly associated with overall survival in GAD patients. The expression levels of ACOX3, HSD17B4 and WHSC1L1 were positively correlated with overall survival (Fig. 6A,D,F), while the expression levels of APOE, DIO2 and NUAK1 were negatively correlated with overall survival (Fig.B,C,E). These MRGs have potential as therapeutic targets in GAD intervention.

4. Discussion

Gastric cancer is a highly heterogeneous cancer. Prognostic guidance based on a classification system is very helpful for clinical management. Currently, the most commonly used clinical classification is pathology-based TNM staging, but there is increasing evidence that GAD patients with the same stage often have different outcomes. Therefore, a more sensitive and specific classification standard is needed. Based on the relationship between gene expression and clinical traits, studies using specific types of genes to construct prognostic models continue to emerge. For example, some researchers have established prognostic models for GAD based on immune-related [17], or tumor microenvironment-related genes [18], etc. All these studies have positive significance for improving the accuracy of prognostic prediction of gastric cancer.

Metabolism-related genes have been used to construct prognostic models in many types of malignancies [19–21]. However, there is currently only one study in gastric cancer that uses MRGs to establish the prognostic model [15] and it is still not perfect with much space for improvement. First, the selection of metabolic genes based on gene set from the MsigDB database is inadequate. The Virtual Metabolic Human (VMH, www.vmh.life) database can provide up to 3695 MRGs [22], which has been used in current study. Secondly, differentially expressed MRGs was selected as input parameters, since several studies have shown that biomarkers based on DEGs between tumors and adjacent

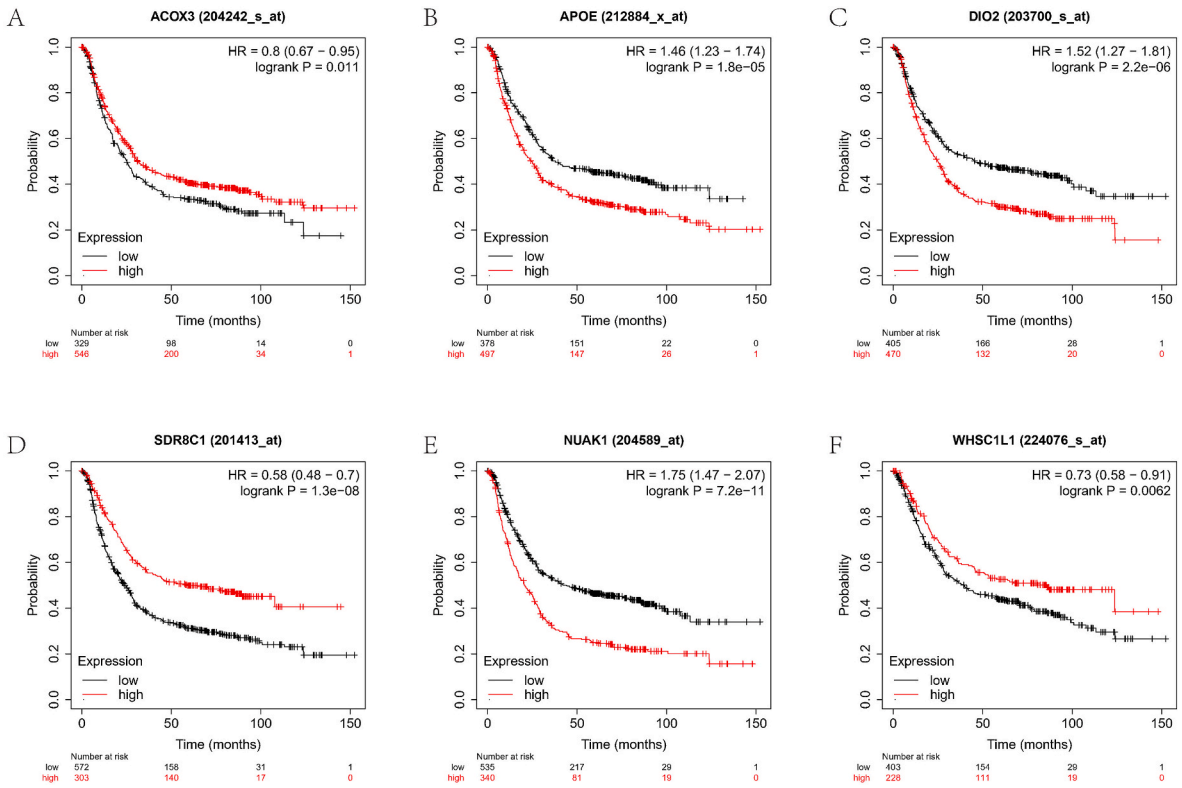

Fig. 6. Validation of the prognostic value of 6 MRGs in GAD by Kaplan-Meier curve. The expressions of ACOX3(A), HSD17B4(D) and WHSC1L1(F) were positively correlated with overall survival, while the expressions of APOE(B), DIO2(C) and NUAK1(E) were negatively correlated with overall survival.

normal tissues can better predict the prognosis of cancer [23,24]. However, in Luo T et al.'s study, the genes for modeling were not screened according to the changes in differential expression. Third, the ROC curve in this study shows that the area under the curve (AUC) of both the training and internal testing cohort is below 0.7, indicating that the model has a poor performance. In our study, we analyzed a total of 520 samples based on three datasets from the GEO database. We first obtained differentially expressed genes between tumor and normal tissues by analyzing the independent GEO datasets, and then intersected MRGs included in the human metabolic database VMH to obtain reliable differentially expressed MRGs.In turn, we constructed a 6 MRGs-based prognostic model for GAD, and the accuracy of the model was confirmed by the external testing cohort. The prediction model established in this study shows good performance and can effectively predict the survival status of patients, which provides a reference for formulating reasonable treatment plans and implementing individualized treatment for patients.

Of these 6 hub MRGs, many have been shown to play an important role in the development and progression of malignancies. Among them, ACOX3 may be a susceptibility gene for cervical cancer and is a potential risk marker [25]; APOE was considered to be an anti-angiogenic and metastatic inhibitor since one study found that tumor-secreted APOE inhibited invasive and metastatic endothelial recruitment by binding LRP1 and LRP8 receptors in melanoma cells [26]; DIO2 may promote the growth of intestinal tumors [27]; HSD17B4 is a potential biomarker for the diagnosis of prostate cancer [28]; NUAK1 was found to be upregulated in both ovarian cancer and nasopharyngeal cancer, and is a potential prognostic marker [29,30]; WHSC1L1 is believed to be an integral part of the oncogenic complex and plays a key role in the pathogenesis of many cancers [31].

The expression profile of these hub MRGs was also verified in protein level through HPA database. Since DIO2 had the most significant relationship with prognosis, we specifically analyzed its protein expression in GAD samples by immunohistochemistry. IHC results showed that the DIO2 was mainly localized in the cytoplasm of cells. Compared with normal gland cells, the expression of DIO2 was enhanced not only in GAD tumor cells but also in reactive hyperplasia gland cells. This indicated that the expression of DIO2 may play a role in the proliferation of abnormal gastric cells, which was also verified by KI67 staining-a nuclear antigen that assesses the ability of cells to proliferate [32]. In the future, we plan to collect more clinical samples to study the expression characteristics of DIO2 in tissues of GAD patients with different pathological stages, and to explore whether DIO2 can be used as a molecular marker for pathological classification of GAD. In particular, it is necessary to study the signaling pathways related to DIO2 and abnormal cell proliferation to provide molecular targets for tumor targeted intervention.

However, there are still shortcomings in this study. First, the metabolism-related prognostic model proposed in this study needs more clinical practice to verify its accuracy. Second, 6 hub MRGs were found in this study, and only immunohistochemical experiments were carried out to detect their expressions in GAD tissues. In the future, cell functional experiments are needed to confirm its role in the development of GAD, which will not only help to understand the metabolic regulation in tumorigenesis but also provide molecular explanations for the established prognostic model.

5. Conclusions

In conclusion, this study established a prognostic model of GAD based on metabolically related genes with considerable predictive power. This study also revealed a group of key metabolic genes involved in the development of GAD, contributing to the understanding of the role of metabolic regulation in tumorigenesis. These findings not only provide a new method for clinical prediction of the prognosis of GAD patients, but also render potential therapeutic intervention targets.

Authorship

WY conceived and directed the study. WY and JZ designed the experimental scheme and analysis protocol. JZ, YL, QC, RH, ZJR, LL and HQW conducted data collation and analysis. WY, HW, HD and JZ discussed, explained the results and wrote the paper. All authors agreed to submit this manuscript for publication.

Ethics approval and informed consent statement

This study was approved by the institutional ethics review committee of Hefei Institutes of Physical Science, Chinese Academy of Sciences. All methods were carried out in accordance with relevant guidelines and regulations.

Availability of data and materials

The datasets presented in this study can be found in online repositories, as mentioned in the "Materials and Methods" section. All data related to this study are available from the corresponding author upon reasonable request.

Funding statement

This study was supported by the National Natural Science Foundation of China (81872276 and 61973295), Research Project issued by Shanxi Scholarship Council of China (2020–085), Scientific and Technologial Innovation Programs of Higher Education Institutions in Shanxi (20121005), and Foundation of Anhui Province Key Laboratory of Medical Physics and Technology (LMPT201908).

Declaration of competing interest

The authors declare that the research was conducted in the absence of any commercial or financial relationships that could be construed as a potential conflict of interest.

Data availability

The data that has been used is confidential.

Acknowledgement

We are grateful to the GEO database for providing a platform for researchers, and to the data contributors for generously sharing their important and meaningful datasets.

Appendix A. Supplementary data

Supplementary data to this article can be found online at https://doi.org/10.1016/j.bbrep.2023.101440.

References

[1] H. Sung, J. Ferlay, R.L. Siegel, M. Laversanne, I. Soerjomataram, A. Jemal, F. Bray, Global cancer statistics 2020: GLOBOCAN estimates of incidence and mortality worldwide for 36 cancers in 185 countries, CA A Cancer J. Clin. 71 (3) (2021) 209–249.

[2] R.S. Zheng, K.X. Sun, S.W. Zhang, H.M. Zeng, X.N. Zou, R. Chen, X.Y. Gu, W. W. Wei, J. He, [Report of cancer epidemiology in China, 2015], Zhonghua Zhongliu Zazhi 41 (1) (2019) 19–28.

[3] J.A. Ajani, J. Lee, T. Sano, Y.Y. Janjigian, D. Fan, S. Song, Gastric adenocarcinoma, Nat. Rev. Dis. Prim. 3 (2017), 17036.

[4] C. Li, S.J. Oh, S. Kim, W.J. Hyung, M. Yan, Z.G. Zhu, S.H. Noh, Macroscopic Borrmann type as a simple prognostic indicator in patients with advanced gastric cancer, Oncology 77 (3–4) (2009) 197–204.

[5] S.H. Noh, S.R. Park, H.K. Yang, H.C. Chung, I.J. Chung, S.W. Kim, H.H. Kim, J. H. Choi, H.K. Kim, W. Yu, J.I. Lee, D.B. Shin, J. Ji, J.S. Chen, Y. Lim, S. Ha, Y. J. Bang, Adjuvant capecitabine plus oxaliplatin for gastric cancer after D2 gastrectomy (CLASSIC): 5-year follow-up of an open-label, randomised phase 3 trial, Lancet Oncol. 15 (12) (2014) 1389–1396.

[6] C. Mariette, F. Carneiro, H.I. Grabsch, R.S. van der Post, W. Allum, G. de Manzoni, Consensus on the pathological definition and classification of poorly cohesive gastric carcinoma, Gastric Cancer 22 (1) (2019) 1–9.

[7] A. Takeno, I. Takemasa, S. Seno, M. Yamasaki, M. Motoori, H. Miyata, K. Nakajima, S. Takiguchi, Y. Fujiwara, T. Nishida, T. Okayama, K. Matsubara, Y. Takenaka, H. Matsuda, M. Monden, M. Mori, Y. Doki, Gene expression profile prospectively predicts peritoneal relapse after curative surgery of gastric cancer, Ann. Surg Oncol. 17 (4) (2010) 1033–1042.

[8] Y. Jiang, Q. Zhang, Y. Hu, T. Li, J. Yu, L. Zhao, G. Ye, H. Deng, T. Mou, S. Cai, Z. Zhou, H. Liu, G. Chen, G. Li, X. Qi, ImmunoScore signature: a prognostic and predictive tool in gastric cancer, Ann. Surg. 267 (3) (2018) 504–513.

[9] M. Kim, S.Y. Rha, Prognostic index reflecting genetic alteration related to disease-free time for gastric cancer patient, Oncol. Rep. 22 (2) (2009) 421–431.

[10] J.Y. Cho, J.Y. Lim, J.H. Cheong, Y.Y. Park, S.L. Yoon, S.M. Kim, S.B. Kim, H. Kim, S. W. Hong, Y.N. Park, S.H. Noh, E.S. Park, I.S. Chu, W.K. Hong, J.A. Ajani, J.S. Lee, Gene expression signature-based prognostic risk score in gastric cancer, Clin. Cancer Res. 17 (7) (2011) 1850–1857.

[11] D. Hanahan, R.A. Weinberg, Hallmarks of cancer: the next generation, Cell 144 (5) (2011) 646–674.

[12] N. Guaragnella, S. Giannattasio, L. Moro, Mitochondrial dysfunction in cancer chemoresistance, Biochem. Pharmacol. 92 (1) (2014) 62–72.

[13] V. Tugnoli, A. Mucci, L. Schenetti, V. Righi, C. Calabrese, A. Fabbri, G. Di Febo, M. R. Tosi, Ex vivo HR-MAS Magnetic Resonance Spectroscopy of human gastric adenocarcinomas: a comparison with healthy gastric mucosa, Oncol. Rep. 16 (3) (2006) 543–553.

[14] M.F. Leal, J. Chung, D.Q. Calcagno, P.P. Assumpção, S. Demachki, I.D. da Silva, R. Chammas, R.R. Burbano, M. de Arruda Cardoso Smith, Differential proteomic analysis of noncardia gastric cancer from individuals of northern Brazil, PLoS One 7 (7) (2012), e42255.

[15] T. Luo, Y. Li, R. Nie, C. Liang, Z. Liu, Z. Xue, G. Chen, K. Jiang, Z.X. Liu, H. Lin, C. Li, Y. Chen, Development and validation of metabolism-related gene signature in prognostic prediction of gastric cancer, Comput. Struct. Biotechnol. J. 18 (2020) 3217–3229.

[16] M. Uhlen, C. Zhang, S. Lee, E. Sjöstedt, L. Fagerberg, G. Bidkhori, R. Benfeitas, M. Arif, Z. Liu, F. Edfors, K. Sanli, K. von Feilitzen, P. Oksvold, E. Lundberg, S. Hober, P. Nilsson, J. Mattsson, J.M. Schwenk, H. Brunnström, B. Glimelius, T. Sjöblom, P.H. Edqvist, D. Djureinovic, P. Micke, C. Lindskog, A. Mardinoglu, F. Ponten, A pathology atlas of the human cancer transcriptome, Science 357 (6352) (2017).

[17] M. Wu, Y. Xia, Y. Wang, F. Fan, X. Li, J. Song, J. Ding, Development and validation of an immune-related gene prognostic model for stomach adenocarcinoma, Biosci. Rep. 40 (10) (2020).

[18] W.Y. Cai, Z.N. Dong, X.T. Fu, L.Y. Lin, L. Wang, G.D. Ye, Q.C. Luo, Y.C. Chen, Identification of a tumor microenvironment-relevant gene set-based prognostic signature and related therapy targets in gastric cancer, Theranostics 10 (19) (2020) 8633–8647.

[19] S. Yu, X. Wang, L. Zhu, P. Xie, Y. Zhou, S. Jiang, H. Chen, X. Liao, S. Pu, Z. Lei, B. Wang, Y. Ren, A systematic analysis of a potential metabolism-related prognostic signature for breast cancer patients, Ann. Transl. Med. 9 (4) (2021) 330.

[20] C. Tang, J. Ma, X. Liu, Z. Liu, Identification of a prognostic signature of nine metabolism-related genes for hepatocellular carcinoma, PeerJ 8 (2020), e9774.

[21] Z. Wang, K.S. Embaye, Q. Yang, L. Qin, C. Zhang, L. Liu, X. Zhan, F. Zhang, X. Wang, S. Qin, Establishment and validation of a prognostic signature for lung adenocarcinoma based on metabolism-related genes, Cancer Cell Int. 21 (1) (2021) 219.

[22] A. Noronha, J. Modamio, Y. Jarosz, E. Guerard, N. Sompairac, G. Preciat, A. D. Daníelsdóttir, M. Krecke, D. Merten, H.S. Haraldsdóttir, A. Heinken, L. Heirendt, S. Magnúsdóttir, D.A. Ravcheev, S. Sahoo, P. Gawron, L. Friscioni, B. Garcia, M. Prendergast, A. Puente, M. Rodrigues, A. Roy, M. Rouquaya, L. Wiltgen, A. Žagare, E. John, M. Krueger, I. Kuperstein, A. Zinovyev, R. Schneider, R.M. T. Fleming, I. Thiele, The Virtual Metabolic Human database: integrating human and gut microbiome metabolism with nutrition and disease, Nucleic Acids Res. 47 (D1) (2019) D614–d624.

[23] X. Gan, M. Guo, Z. Chen, Y. Li, F. Shen, J. Feng, W. Cai, B. Xu, Development and validation of a three-immune-related gene signature prognostic risk model in papillary thyroid carcinoma, J. Endocrinol. Invest. 44 (10) (2021) 2153–2163.

[24] P.F. Chen, Q.H. Li, L.R. Zeng, X.Y. Yang, P.L. Peng, J.H. He, B. Fan, A 4-gene prognostic signature predicting survival in hepatocellular carcinoma, J. Cell. Biochem. 120 (6) (2019) 9117–9124.

[25] H. Lin, Y. Ma, Y. Wei, H. Shang, Genome-wide analysis of aberrant gene expression and methylation profiles reveals susceptibility genes and underlying mechanism of cervical cancer, Eur. J. Obstet. Gynecol. Reprod. Biol. 207 (2016) 147–152.

[26] N. Pencheva, H. Tran, C. Buss, D. Huh, M. Drobnjak, K. Busam, S.F. Tavazoie, Convergent multi-miRNA targeting of ApoE drives LRP1/LRP8-dependent melanoma metastasis and angiogenesis, Cell 151 (5) (2012) 1068–1082.

[27] Y. Kojima, Y. Kondo, T. Fujishita, E. Mishiro-Sato, R. Kajino-Sakamoto, M. M. Taketo, M. Aoki, Stromal iodothyronine deiodinase 2 (DIO2) promotes the growth of intestinal tumors in Apc(Δ716) mutant mice, Cancer Sci. 110 (8) (2019) 2520–2528.

[28] H. Huang, R. Liu, Y. Huang, Y. Feng, Y. Fu, L. Chen, Z. Chen, Y. Cai, Y. Zhang, Y. Chen, Acetylation-mediated degradation of HSD17B4 regulates the progression of prostate cancer, Aging (Albany NY) 12 (14) (2020) 14699–14717.

[29] N.T. Phippen, N.W. Bateman, G. Wang, K.A. Conrads, W. Ao, P.N. Teng, T.A. Litzi, J. Oliver, G.L. Maxwell, C.A. Hamilton, K.M. Darcy, T.P. Conrads, NUAK1 (ARK5) is associated with poor prognosis in ovarian cancer, Front. Oncol. 6 (2016) 213.
[30] J. Liu, G. Tang, H. Huang, H. Li, P. Zhang, L. Xu, Expression level of NUAK1 in human nasopharyngeal carcinoma and its prognostic significance, Eur. Arch. Oto-Rhino-Laryngol. 275 (10) (2018) 2563–2573.
[31] X. Han, L. Piao, Q. Zhuang, X. Yuan, Z. Liu, X. He, The role of histone lysine methyltransferase NSD3 in cancer, OncoTargets Ther. 11 (2018) 3847–3852.
[32] T. Scholzen, J. Gerdes, The Ki-67 protein: from the known and the unknown, J. Cell. Physiol. 182 (3) (2000) 311–322.